Ecography

ECOG-03641
Read, Q. D., Grady, J. M., Zarnetske, P. L., Record, S., Baiser, B., Belmaker, J., Tuanmu, M.-N., Strecker, A., Beaudrot, L. and Thibault, K. M. 2018. Among-species overlap in rodent body size distributions predicts species richness along a temperature gradient. – Ecography doi: 10.1111/ecog.03641

Supplementary material

Appendix 1: Site Information

Site code	*Site name*	*U.S. state*	*Latitude*	*Longitude*	*Elevation (m)*
BART	Bartlett Experimental Forest	NH	44.06	-71.29	378
BLAN	Blandy Experimental Farm	VA	39.07	-78.01	157
CPER	Central Plains Experimental Range	CO	40.82	-104.73	1644
GRSM	Great Smoky Mountains National Park, Twin Creeks	TN	35.68	-83.50	730
HARV	Harvard Forest	MA	42.47	-72.22	253
JERC	Jones Ecological Research Center	GA	31.19	-84.47	42
JORN	Jornada LTER	NM	32.60	-106.83	1324
OAES	Klemme Range Research Station	OK	35.41	-99.06	512
KONZ	Konza Prairie Biological Station	KS	39.10	-96.57	396
MOAB	Moab	UT	38.25	-109.39	1825
NIWO	Niwot Ridge Mountain Research Station	CO	40.05	-105.57	3343
STER	North Sterling	CO	40.47	-103.02	1361
ORNL	Oak Ridge	TN	35.95	-84.29	293
ONAQ	Onaqui-Ault	UT	40.18	-112.47	1724
OSBS	Ordway-Swisher Biological Station	FL	29.69	-81.98	35
SCBI	Smithsonian Conservation Biology Institute	VA	38.89	-78.15	352
SERC	Smithsonian Environmental Research Center	MD	38.89	-76.55	13
STEI	Steigerwaldt Land Services	WI	45.74	-89.97	499
TALL	Talladega National Forest	AL	32.93	-87.41	119
UKFS	The University of Kansas Field Station	KS	39.04	-95.20	310
TREE	Treehaven	WI	45.49	-89.57	461
UNDE	UNDERC	MI	46.24	-89.53	515
WOOD	Woodworth	ND	47.14	-99.24	586

Site code	*Mean annual temperature (°C)*	*Mean annual precipitation (mm y^{-1})*	*Terrain ruggedness index*	*Observed rodent richness*	*Chao1 richness estimator*	*NLCD land cover class*
BART	5.6	1377	1.383	4	4	Deciduous forest
BLAN	12.2	979	0.421	4	4	Deciduous forest
CPER	8.6	343	0.263	10	10	Grassland/herbaceous
GRSM	12.2	1531	1.665	4	4	Deciduous forest
HARV	7.9	1209	0.634	5	5	Deciduous forest
JERC	19.3	1309	0.217	7	8	Evergreen forest
JORN	15.7	270	0.133	13	13	Shrub/scrub
OAES	15.6	775	0.371	11	11	Grassland/herbaceous
KONZ	12.4	871	1.198	9	9	Grassland/herbaceous
MOAB	10.2	317	0.288	11	14	Shrub/scrub
NIWO	0.1	987	1.572	6	6.33	Evergreen forest
STER	9.7	433	0.120	9	9	Cultivated crops
ORNL	14.5	1330	1.542	5	5	Deciduous forest
ONAQ	8.9	326	0.635	7	7	Shrub/scrub
OSBS	20.9	1306	0.316	6	7	Evergreen forest
SCBI	11.8	1077	1.475	7	8	Deciduous forest
SERC	13.6	1074	0.618	3	3	Deciduous forest
STEI	4.4	797	0.218	6	6	Deciduous forest
TALL	17.2	1377	1.614	4	4	Deciduous forest
UKFS	12.7	991	0.859	5	5	Deciduous forest
TREE	4.8	798	0.310	5	5	Mixed forest
UNDE	4.3	800	0.357	5	5	Woody wetlands
WOOD	4.9	494	0.314	4	4	Grassland/herbaceous

Appendix 2: Rodent Species List

Scientific name	*Number of individuals captured*	*Number of sites where present*	*Mean body mass (g)*	*Standard deviation of body mass*	*Q1 of body mass*	*Q3 of body mass*
Chaetodipus hispidus	268	4	41.92	12.91	34	50
Chaetodipus penicillatus	212	1	16.08	5.90	15	17
Dipodomys merriami	110	1	43.39	4.84	41	46
Dipodomys microps	50	1	61.31	7.95	56.25	66.75
Dipodomys ordii	361	5	58.89	10.89	51	68
Dipodomys spectabilis	22	1	123.34	19.04	115	135
Lemmiscus curtatus	6	1	22.17	3.60	20.25	24.5
Microtus longicaudus	1	1	29.00	—	29	29
Microtus montanus	2	1	22.50	14.85	17.25	27.75
Microtus ochrogaster	181	5	38.11	8.02	34	43
Microtus pennsylvanicus	164	5	33.79	12.69	25	45.25
Microtus pinetorum	7	4	24.67	6.77	24.25	26.5
Mus musculus	101	6	16.48	5.68	12	21
Myodes gapperi	297	6	20.22	5.43	16	24
Napaeozapus insignis	200	5	24.46	5.32	21	27
Neotoma albigula	10	2	123.54	59.36	85	160
Neotoma floridana	96	4	177.90	58.88	143.75	212.25
Neotoma mexicana	5	1	129.17	43.04	111	128.75
Neotoma micropus	5	2	197.25	44.90	150.5	235
Ochrotomys nuttalli	31	4	19.38	3.57	17	21
Oryzomys palustris	1	1	24.00	—	24	24
Perognathus fasciatus	8	2	9.25	5.26	6.75	8.5
Perognathus flavescens	6	3	11.00	1.79	10	11.75
Perognathus flavus	114	4	7.47	1.60	7	8
Perognathus parvus	166	1	18.99	3.35	16	21
Peromyscus boylii	1	1	25.00	—	25	25
Peromyscus gossypinus	206	4	24.63	4.97	21	28
Peromyscus leucopus	983	15	21.27	5.28	18	24
Peromyscus maniculatus	1431	17	18.79	4.06	16	21
Peromyscus merriami	1	1	23.00	—	23	23
Peromyscus polionotus	38	2	13.39	1.97	12	14
Peromyscus truei	14	1	24.62	4.22	23	27
Phenacomys intermedius	2	1	30.00	—	30	30
Podomys floridanus	35	1	33.09	5.45	30	37
Rattus rattus	1	1	180.00	—	180	180

Scientific name	***Number of individuals captured***	***Number of sites where present***	***Mean body mass (g)***	***Standard deviation of body mass***	***Q1 of body mass***	***Q3 of body mass***
Reithrodontomys fulvescens	2	1	9.50	4.95	7.75	11.25
Reithrodontomys humulis	2	2	9.50	4.95	7.75	11.25
Reithrodontomys megalotis	165	5	11.66	2.75	10	13
Reithrodontomys montanus	240	3	11.34	2.42	10	13
Sigmodon hispidus	471	7	101.66	47.62	63	131
Zapus hudsonius	80	8	20.25	5.61	16	23.5
Zapus princeps	28	2	20.58	3.83	18	22

Appendix 3: Species Richness Estimators

We compared richness estimators to diagnose sampling problems. These values are the richness of all target rodent species at each site, with individuals that could not be identified to species (such as "*Peromyscus* sp." or "Rodent sp.") removed. The Chao1 richness estimator was calculated with the formula: $$\text{Chao1} = S_{obs} + \frac{f_1(f_1 - 1)}{2(f_2 + 1)}$$, where S_{obs} is observed richness, f_1 is the number of singletons, and f_2 is the number of doubletons. The asymptotic richness estimator based on Hill numbers was calculated with the function *iNEXT()* provided in the R package iNEXT. Bootstrapped confidence intervals are given around the asymptotic richness estimator. See figures below.

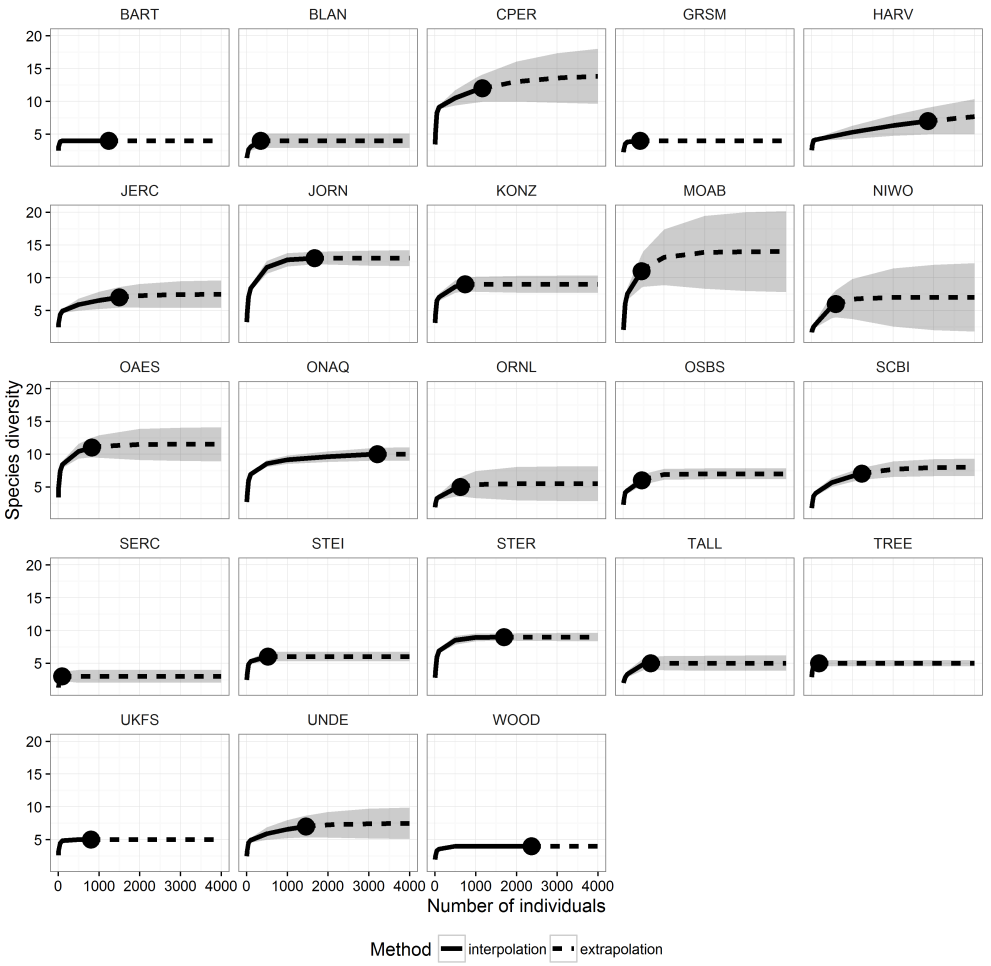

Figure A1. The extrapolated species richness for each of the twenty-three NEON sites. The dotted lines show extrapolation of richness out past the points (the actual observed abundances and richness values). If the asymptote of the extrapolation is not much more than the observed value, we can say that the site is well sampled. A few sites had a number of species with very few individuals, indicating that further sampling would discover more species than were actually observed.

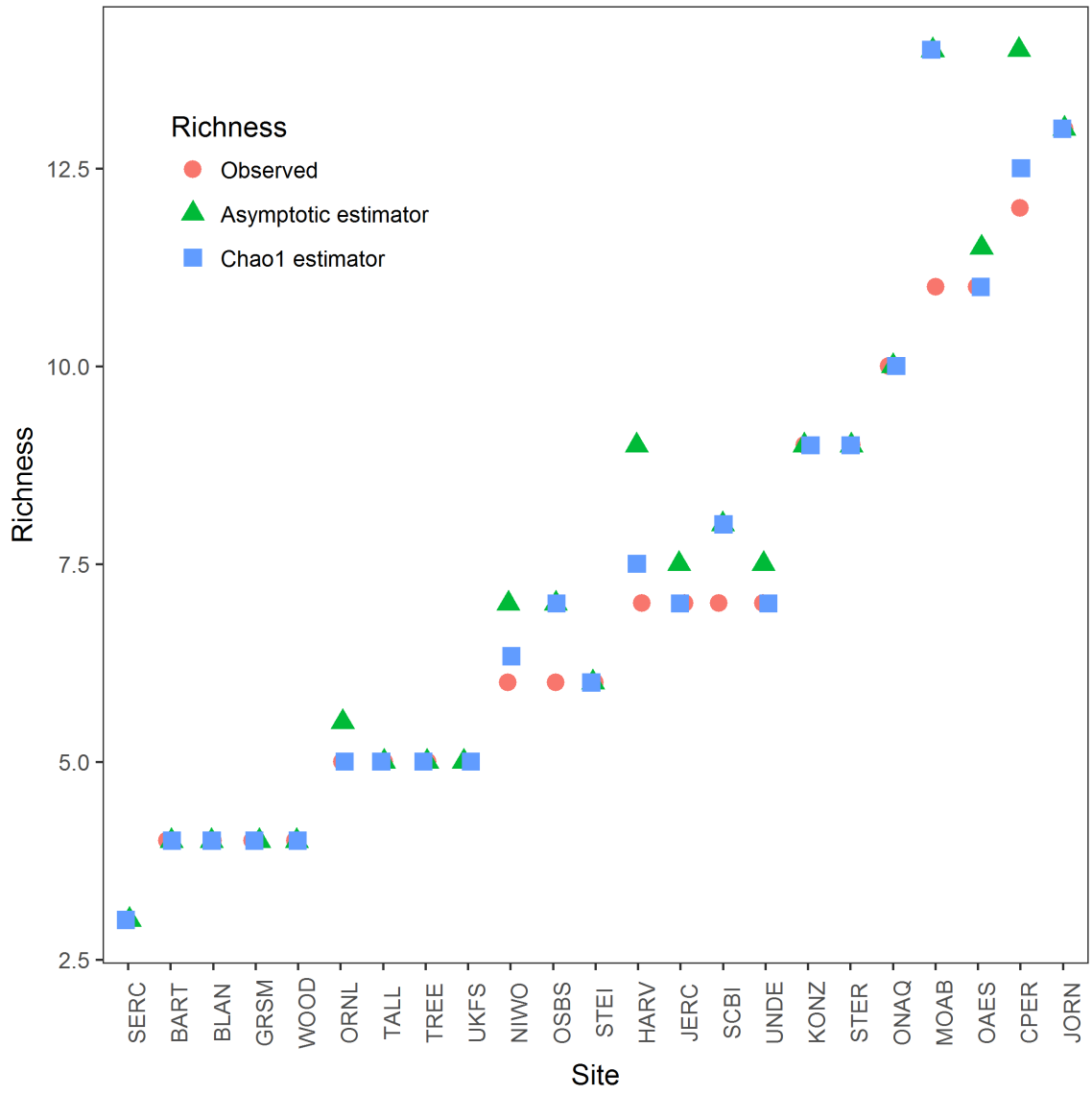

Figure A2. Both asymptotic and Chao1 estimators plotted with the observed richness values. Sites ordered by observed rodent richness.

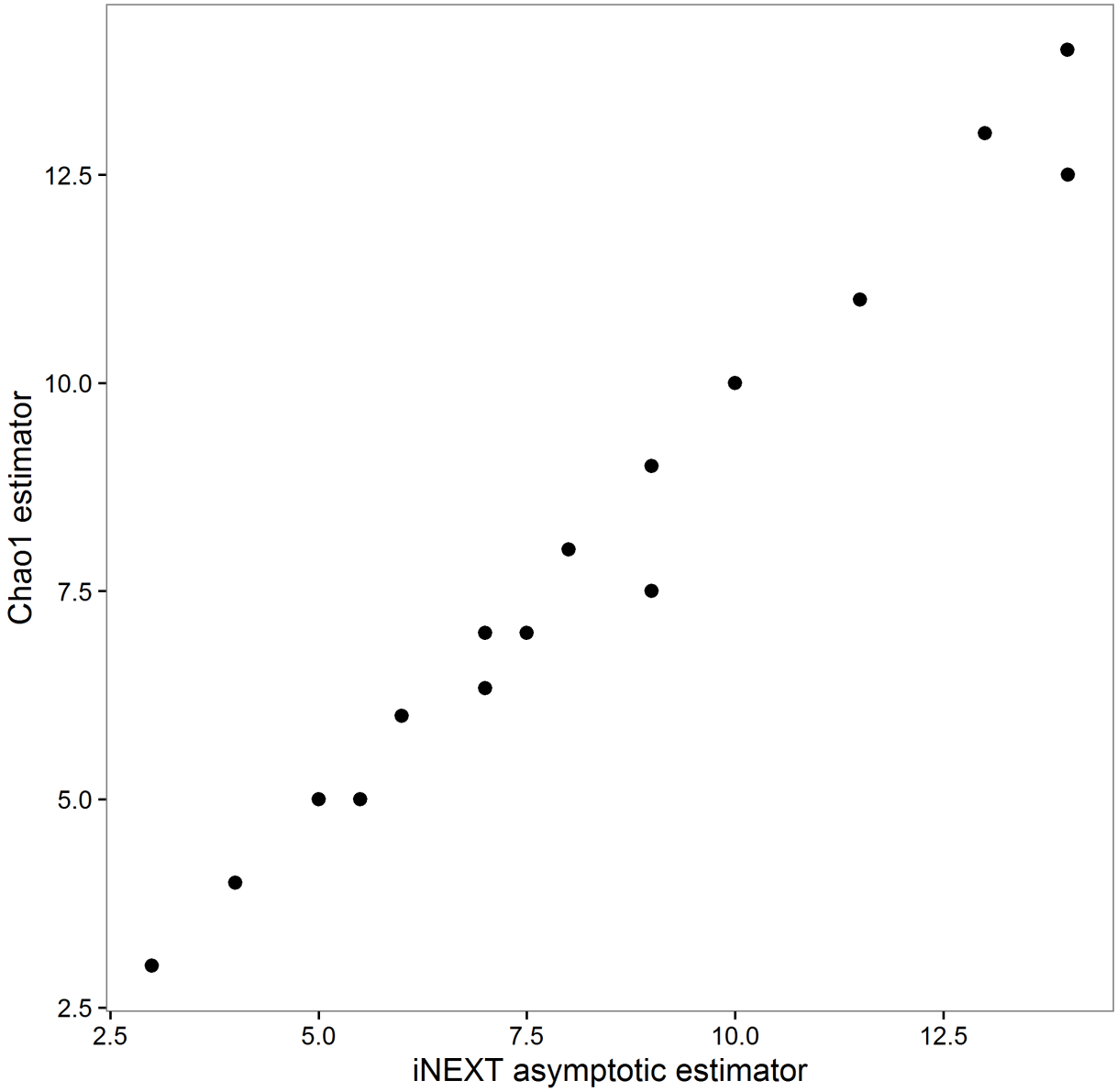

Figure A3. Comparison of the two estimators. They are very similar ($R^2 = 0.98$).

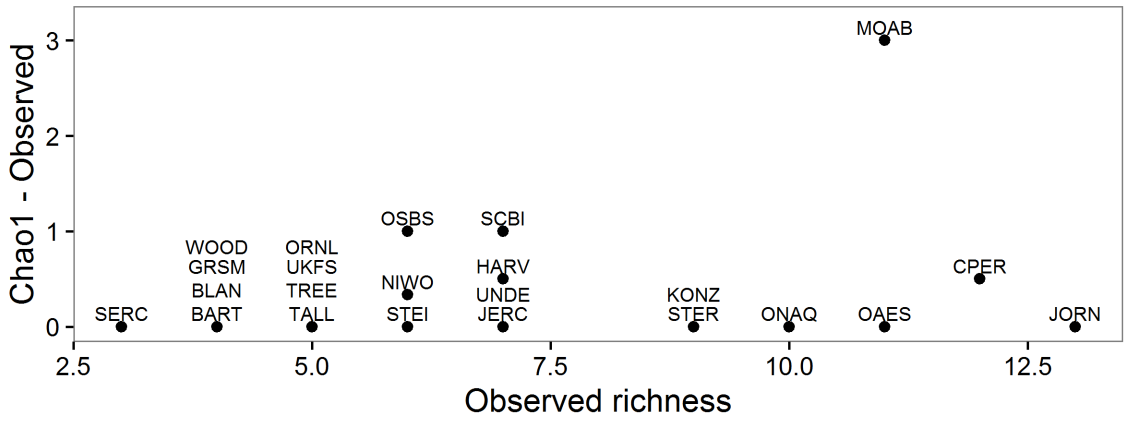

Figure A4. Observed richness plotted on the x-axis, and the difference between the Chao1 richness estimator and observed richness plotted on the y-axis. Most sites have a small difference (<1) between the estimator and observed value, but the Moab community may be undersampled, given the difference of 3 between the estimated and observed values.

Appendix 4: Topographic Heterogeneity and Environmental Heterogeneity

We downloaded data from the National Elevation Database (NED) for each NEON site. For each mammal sampling grid, we calculated the mean elevation, mean slope, mean aspect, terrain ruggedness index, and topographic position index including all NED pixels within the sampling grid (approximately 100 pixels). We calculated these indices using the *terrain()* function in the R package raster.

We also extracted data from the pixels corresponding to the mammal sampling grids from the following data layers from the Moderate-resolution Imaging Spectroradiometer (MODIS) dataset: leaf area index (LAI), fraction of absorbed photosynthetically active radiation (fPAR), normalized difference vegetation index (NDVI), enhanced vegetation index (EVI), net primary productivity (NPP), and gross primary productivity (GPP), for all available dates since 2000, using functions from the R package MODISTools.

We calculated the spatial coefficient of variation for each of the topographical and environmental variables extracted at the level of the NEON site. We ran a principal component analysis using the *prcomp()* function in the base R distribution. The bulk of the variation (70.0%) was explained by the first two axes: PC1 (39.0%) was associated with the MODIS variables and represented within-site spatial heterogeneity in ecosystem productivity and aboveground biomass. PC2 (31.0%) was associated with the topographical variables.

Appendix 5: Structural equation model fits including productivity and plant richness

We fit structural equation models including direct and indirect effects of temperature (T; minimum temperature of the coldest month) and productivity (P; mean annual net primary productivity) on rodent species richness (R; Chao1 estimator of rodent species richness) mediated by body size overlap (O). The equations comprising the full model are below.

$$R = \beta_1 T + \beta_2 P + \beta_3 O$$
$$O = \beta_4 T + \beta_5 P$$

We fit models including all direct and indirect effects, models without the direct effects of temperature and productivity, and models without any effect of productivity (Figure A5).

We also investigated whether plant species richness might be a mechanism influencing body size overlap among co-occurring rodents. We extracted data from a recent global plant biodiversity mapping study (Ellis et al. 2012). A global raster layer containing estimated regional plant richness is available as supplemental material for the above study. We extracted the estimated regional plant richness value in the ~100 km diameter pixel containing each NEON site. We fit two additional models including this variable (represented as R_p), one modeling it as an additional endogenous variable influenced by temperature and influencing overlap, and the other modeling it as an exogenous variable affecting overlap independently of temperature (Figure A6).

We compared the Bayesian Information Criterion of each model, and the proportion of variation in richness that each model explained. As the table below shows, the model selection procedure clearly rejected any models including direct or indirect effects of productivity as adding complexity without appreciably increasing the explanatory power of the model (Figure A5). The same was true for plant richness (Figure A6); adding plant richness as a predictor was not supported, although the indirect effect of plant richness on rodent richness, mediated by overlap, was significant and negative after accounting for the effect of temperature. Because of the lack of support for adding additional variables to the structural equation model, we discuss only the model including the temperature effects in the manuscript. However, it is important to note that these models were fit with data from only 23 sites, so it is unlikely that more than two predictor variables would be supported in any case. It is possible that increased plant diversity increases the number of available diet niches for a given body size, making coexistence of more rodent species with overlapping body sizes possible. This effect, if robust, would be independent of both productivity and climate; we recommend testing this with a study design that has sufficient statistical power to detect the effect.

Work cited: Ellis, E. C. et al. 2012. All is not loss: plant biodiversity in the Anthropocene. - PLOS ONE 7: e30535.

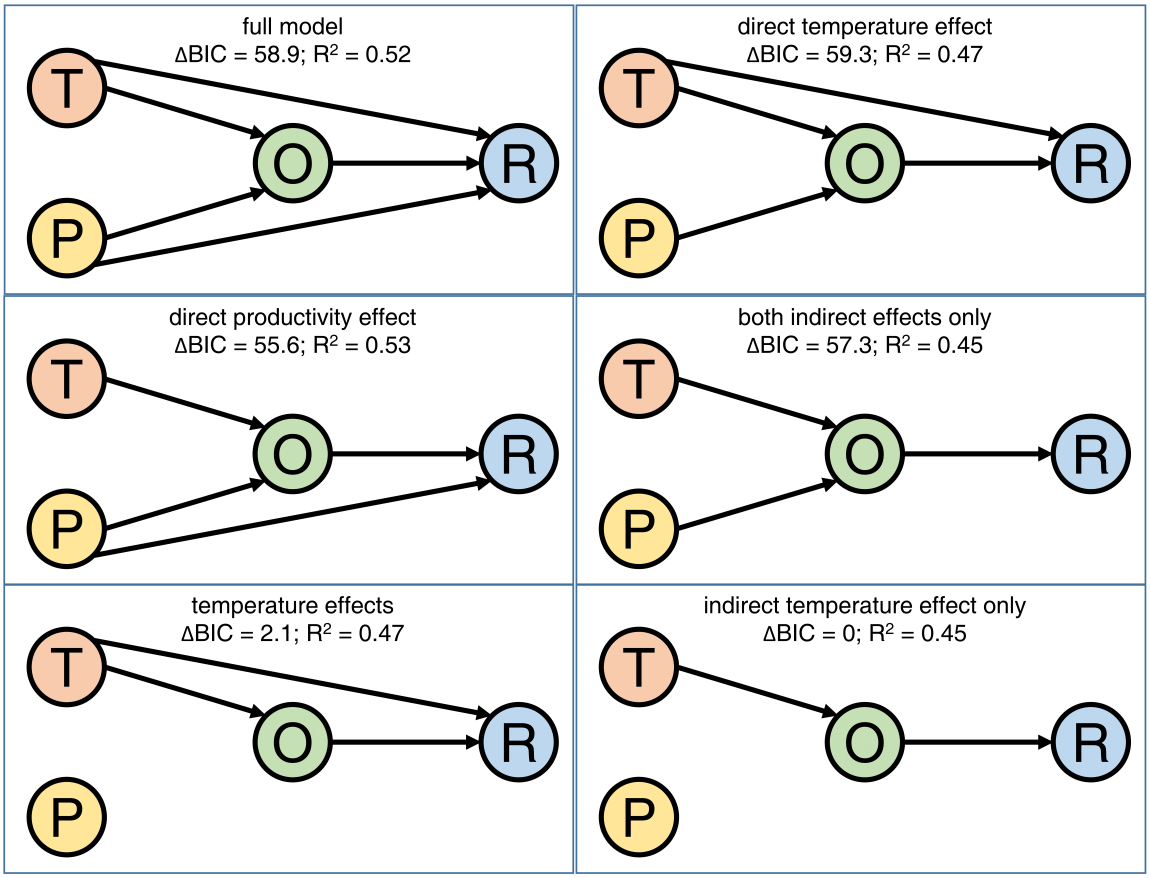
full model
ΔBIC = 58.9; R² = 0.52
T
O
R
P
direct temperature effect
ΔBIC = 59.3; R² = 0.47
T
O
R
P
direct productivity effect
ΔBIC = 55.6; R² = 0.53
T
O
R
P
both indirect effects only
ΔBIC = 57.3; R² = 0.45
T
O
R
P
temperature effects
ΔBIC = 2.1; R² = 0.47
T
O
R
P
indirect temperature effect only
ΔBIC = 0; R² = 0.45
T
O
R
P

Figure A5.

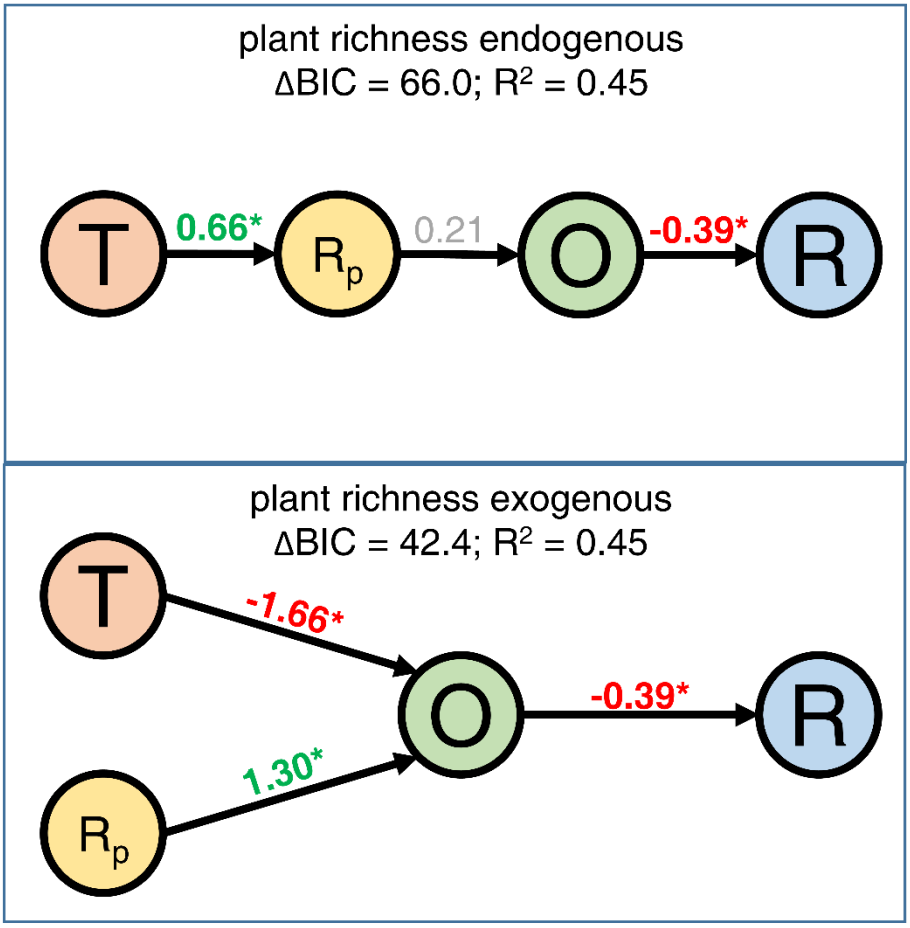

Figure A6. Two ways to model the effect of plant richness on rodent richness, mediated by overlap. Terms for which the credible interval does not overlap zero are in bold with an asterisk. Note that in the model at bottom, plant richness is positively related to rodent body size overlap, indicating that increased plant richness leads to less among-species differentiation in body size, after accounting for the effect of temperature.

Appendix 6: Density plots for all sites

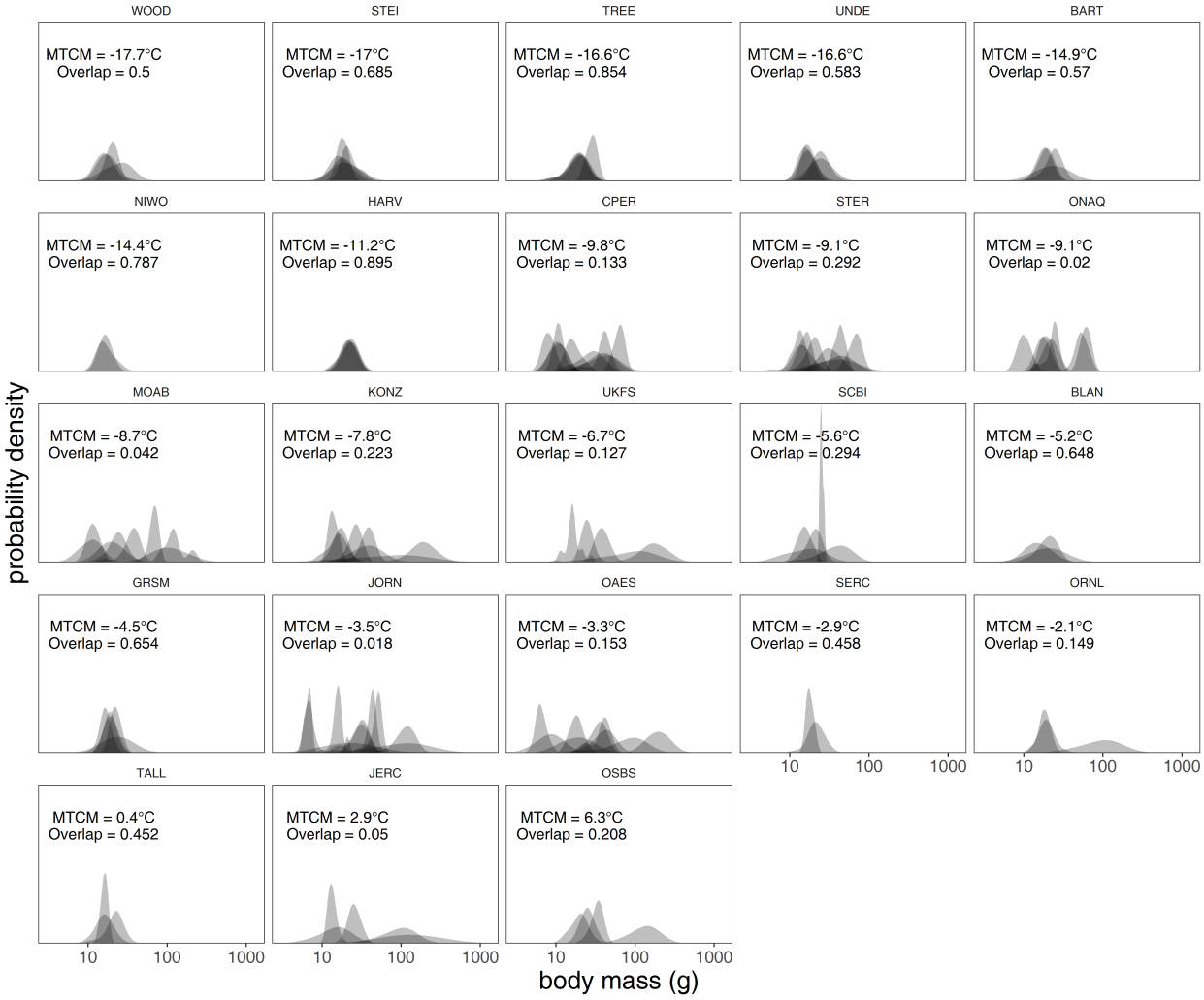

Figure A7. The observed density plots for each of the 23 sites, shaded to show where trait overlap is highest. The individual sites' density plots are ordered by the minimum temperature of the coldest month (MTCM), and the median overlap value is given on each plot, as well as the MTCM.